Computation of Steady and Unsteady Vortex-Dominated Flows with Shock Waves

Osama A. Kandil* and H. Andrew Chuang†
Old Dominion University, Norfolk, Virginia

The unsteady Euler equations have been derived in the conservation form for the flow relative motion with respect to a rotating frame of reference. The resulting equations are solved by using a central-difference finite-volume scheme with four-stage Runge-Kutta time stepping. For steady flow applications local time stepping is used, and for unsteady applications the minimum global time stepping is used. A three-dimensional fully vectorized computer program has been developed and applied to steady and unsteady maneuvering delta wings. The capability of the three-dimensional program has been demonstrated for a rigid sharp-edged delta wing undergoing uniform rolling in a conical flow and rolling oscillations in a locally conical flow.

Introduction

PREDICTION of the steady and unsteady vortex-dominated flows around delta and delta-like wings is of paramount importance for the analysis and design of modern and future fighter aircraft under combat and maneuvering conditions. Over wide ranges of variation of the normal Mach number, normal angle of attack, and sweepback angle, complex flows develop. These flows include large- and small-scale vortices, strong and weak shock waves that may occur below and/or above the large-scale vortices, and shock-induced separations.[1]

Explicit and implicit computational schemes for steady vortex-dominated flows that use psuedotime integration of the unsteady Euler and Navier-Stokes equations[2-12] have been developed and successfully used to predict many types of these flows. A comprehensive review of the state-of-the-art of the Computational Fluid Dynamics (CFD) of steady vortex-dominated flows is given by Newsome and Kandil.[12] Although a substantial research work is currently progressing to improve and extend the computational schemes for steady flows, there is a serious lack of research effort to extend and apply the existing CFD schemes to the unsteady three-dimensional vortex-dominated problems, which are vital for aeroelastic and dynamic applications for supermaneuvering aircraft. The shortage is attributed to the computational cost associated with the time-accurate solution of the problem and the grid motion and deformation.

The majority of the existing unsteady computational applications is in the area of unsteady transonic flow, which has been of special interest to researchers in the area of aeroelasticity for flutter prediction. In the unsteady transonic flow area, most of the available computational schemes are based on the time-accurate solution of the transonic small disturbance (TSD) equation[14,15] and the time-accurate solution of the full-potential (FP) equation.[16-18] Neither the TSD equation nor the FP equation can treat flows with strong shock waves or vortex-dominated flows. Very recently, time-accurate solutions of the Euler[19-21] and Navier-Stokes equations[22,23] have been presented with applications to two-dimensional unsteady transonic airfoil flows. A recent comprehensive review of the state-of-the-art of the computational unsteady transonic flows has been given by Edwards and Thomas[23] from the perspective of aeroelastic applications.

Unsteadiness in the flows may originate from the time-dependent rigid-body translation (e.g., forward acceleration and heaving oscillations) and rotation (e.g., rolling, pitching, and yawing oscillations), aeroelastic deformations and/or flow instabilities (e.g., vortex breakdown, wing rocking, and transition to turbulence), among others. These sources of flow unsteadiness exist in maneuvering conditions of delta wings over a wide range of Mach numbers. Obviously, the CFD area has not matured enough to address all of these issues simultaneously. However, research effort is currently progressing in that direction, and dealing with each individual issue separately.

In the present paper, we address the problem of unsteady vortex-dominated flows with shock waves of a maneuvering delta wing through the time-accurate solution of Euler equations of the flow relative motion in a moving frame of reference. A three-dimensional, fully vectorized computer program, which uses a central-difference finite-volume scheme with four-stage Runge-Kutta time stepping, has been developed. Since at this time we have limited computer resources, and since most of the flow characteristics and physics can be obtained through the solution of the conical flow problem, we used the three-dimensional program to solve two conical flow problems of a sharp-edged delta wing. The first problem is that of a uniform rolling in a conical flow, and the second is that of a rolling oscillation in a locally conical flow. To the best of our knowledge, this is the first time such a problem is considered by using Euler equations.

The present formulation is not restricted to any particular motion and can be easily extended to include aeroelastic deformation. With minimum effort, the viscous terms can be included for thin-layer or full Navier-Stokes solutions. The formulation in terms of the moving frame of reference with a rigidly moving grid saves a large percentage of the computational time, since the computation of the grid motion for rigid wings is not needed. For aeroelastic deformations of the wing, which are usually small, the frequency of grid deformation calculations will only be required after substantial numbers of time steps.

Formulation

The conservation form of the unsteady Euler equations for the absolute motion of the flow in a space-fixed frame of

Received June 1, 1987; revision received Nov. 25, 1987.

*Professor, Department of Mechanical Engineering and Mechanics. Associate Fellow AIAA.

†Research Assistant, Department of Mechanical Engineering and Mechanics. Member AIAA.

reference is given by

$$\frac{\partial \rho}{\partial t} + \nabla \cdot (\rho V) = 0 \tag{1}$$

$$\frac{\partial (\rho V)}{\partial t} + \nabla \cdot (\rho VV + p\bar{\bar{I}}) = 0 \tag{2}$$

$$\frac{\partial (\rho e)}{\partial t} + \nabla \cdot (\rho h V) = 0 \tag{3}$$

$$e = \frac{p}{\rho(\gamma - 1)} + \frac{V^2}{2} \tag{4}$$

$$h = e + (p/\rho) \tag{5}$$

where ρ is the density, V the flow velocity vector, p the pressure, $\bar{\bar{I}}$ the unit tensor, e and h the total energy and total enthalpy per unit mass, and γ the ratio of specific heats.

To express these equations in terms of a moving frame of reference, we use the following relations of the substantial and local derivatives for a scalar a and a vector A:

$$\frac{Da}{Dt} = \frac{D'a}{Dt'} \tag{6a}$$

$$\frac{\partial a}{\partial t} = \frac{\partial' a}{\partial t'} - V_t \cdot \nabla a \tag{6b}$$

$$\frac{DA}{Dt} = \frac{D'A}{Dt'} + \bar{\omega} x A \tag{7a}$$

$$\frac{\partial A}{\partial t} = \frac{\partial' A}{\partial t'} - V_t \cdot \nabla A + \bar{\omega} x A \tag{7b}$$

Equations (6) and (7) express the substantial and local derivatives in the space-fixed frame in terms of their counterparts in the moving frame of reference. In Eqs. (6) and (7), $\bar{\omega}$ is the moving-frame angular velocity, V_t the transformation velocity from the absolute to the relative motion, and the prime refers to the derivatives with respect to the moving frame. The transformation velocity V_t, which is the difference between the absolute V and relative V_r velocities of the flow, is a function of the moving frame of reference translation and rotation, and hence is given by

$$V_t = V - V_r = V_o + \bar{\omega} x r \tag{8}$$

where V_o is the translation velocity and r the position vector of the fluid particle with respect to the moving frame of reference.

If Eqs. (6) and (7) are substituted into Eqs. (1-3), the resulting equations express the absolute motion of the flow with respect to the moving frame of reference. Unfortunately, these equations cannot be written in the conservation form for the computational scheme. On the other hand, if Eqs. (6) and (7) along with $V = V_r + V_t$ are substituted into Eqs. (1-3), the resulting equations express the relative motion of the flow with respect to the moving frame. These equations are in the conservation form, and hence they are preferred for the computational scheme. Restricting the motion of the frame of reference to the rotational motion (for the present applications), i.e., $V_o = 0$ and $DV_o/Dt = 0$, we obtain the equations of relative motion in the rotating frame of reference:

$$\frac{\partial' \rho}{\partial t'} + \nabla \cdot (\rho V_r) = 0 \tag{9}$$

$$\frac{\partial' (\rho V_r)}{\partial t'} + \nabla \cdot [\rho V_r V_r + p\bar{\bar{I}}] = -\rho[\dot{\bar{\omega}} x r + 2\bar{\omega} x V_r + \bar{\omega} x (\bar{\omega} x r)] \tag{10}$$

$$\frac{\partial' (\rho e_r)}{\partial t'} + \nabla \cdot [\rho h_r V_r] = -\rho[V_r \cdot (\dot{\bar{\omega}} x r) + (\bar{\omega} x r) \cdot (\dot{\bar{\omega}} x r)] \tag{11}$$

where

$$e_r = \frac{p}{\rho(\gamma - 1)} + \frac{V_r^2}{2} - \frac{1}{2} |\bar{\omega} x r^2| = e - V \cdot (\bar{\omega} x r) \tag{12}$$

$$h_r = \frac{\gamma p}{\rho(\gamma - 1)} + \frac{V_r^2}{2} - \frac{1}{2} |\bar{\omega} x r^2| = h - V \cdot (\bar{\omega} x r) \tag{13}$$

The last equation of h_r gives the rothalpy of the flow.

Method of Solution

The abstract conservative form of the unsteady flow relative motion in terms of the rotating coordinates (x', y', z') is given by

$$\frac{\partial' \bar{q}_r}{\partial t'} + \frac{\partial' \bar{E}_r}{\partial x'} + \frac{\partial' \bar{F}_r}{\partial y'} + \frac{\partial' \bar{G}_r}{\partial z'} = \bar{S} \tag{14}$$

where

$$\bar{q}_r = [\rho, \rho u_r, \rho v_r, \rho w_r, \rho e_r]^t \tag{15}$$

$$\bar{E}_r = [\rho u_r, \rho u_r^2 + p, \rho u_r v_r, \rho u_r w_r, \rho u_r h_r]^t \tag{16}$$

$$\bar{F}_r = [\rho v_r, \rho u_r v_r, \rho v_r^2 + p, \rho v_r w_r, \rho v_r h_r]^t \tag{17}$$

$$\bar{G}_r = [\rho w_r, \rho u_r w_r, \rho v_r w_r, \rho w_r^2 + p, \rho w_r h_r]^t \tag{18}$$

$$\bar{S} = [0, 0, \rho(\dot{\omega} z' + 2\omega w_r + \omega^2 y') - \rho(\dot{\omega} y' + 2\omega v_r - \omega^2 z') - \rho\dot{\omega}(-v_r z' + w_r y' + \omega y'^2 + \omega z'^2)]^t \tag{19}$$

Since only the rolling motion is solved in this paper, the source term $\bar{S}$ has been written for $\bar{\omega} = \omega \bar{e}_{x'}$, and $\dot{\bar{\omega}} = \dot{\omega} \bar{e}_{x'}$. It should be noted that if $\bar{\omega} = \dot{\bar{\omega}} = 0$, $V_r = V$, Eqs. (12-19) reduce to Eqs. (1-5) of the absolute motion. Hence, any computational scheme and the corresponding computer program can be easily converted to solve the set of Eqs. (12-19).

In this paper we use the central-difference finite-volume scheme with Runge-Kutta time stepping to solve Eqs. (12-19). The details of the scheme have been covered earlier by the authors in Refs. 4 and 9 and, therefore, they are not covered here. The three-dimensional fully vectorized computer program that was developed by the authors in Ref. 9 has been modified to include the rotational motion of the frame of reference. Moreover, since we are dealing with asymmetric flows in general, the symmetric flow condition has been removed, and the computational domain covers both sides of the geometrical plane of symmetry.

Exact and Locally Conical Flows

Because of the limited computational resources we have at this time, we decided to solve the conical flow problems using the three-dimensional program. Conical flow problems are computationally economical and include almost all the physics of the corresponding three-dimensional problems—large- and small-scale vortices, weak and strong shocks, shock-induced separations, and the interactions of all these regions.

If the conical coordinates $\xi' = x'$, $\eta' = y/x'$, and $\zeta' = z/x'$ are used to transform the relative motion equations, Eqs. (14-19), the resulting equations will not represent a conical flow. On the other hand, if the conical coordinates are used to transform the absolute motion equations, Eqs. (1-5), the resulting equations will represent an exact conical flow for steady-flow problems. For the unsteady-flow problems, the resulting equations can be made "locally conical" if they are solved at a fixed axial location.

In a three-dimensional computer program, conical flow solutions can be obtained by forcing the flow vector field of the absolute motion to be equal in three successive conical planes $i-1$, i and $i+1$; $i=2$. These conditions are given by

$$\rho_{i+1}=\rho_i, \quad (\rho V)_{i+1}=(\rho V)_i, \quad (\rho e)_{i+1}=(\rho e)_i \tag{20}$$

Since the present three-dimensional computer program solves for the relative motion as the basic unknowns, Eq. (20) in terms of the relative motion becomes

$$(\rho V_r)_{i+1}=(\rho V_r)_i+\rho_i\,\dot{\bar{\omega}}x\,(r_i-r_{i+1}) \tag{21}$$

$$(\rho e_r)_{i+1}=(\rho e_r)_i+[(\rho V_r)_i+\rho_i\,\dot{\bar{\omega}}xr_i]\cdot[\dot{\bar{\omega}}x(r_i-r_{i+1})] \tag{22}$$

All of the conical flow problems in this paper are solved at $x'=1$.

Initial Conditions

Different initial conditions are used depending on the problem under consideration. For a symmetric steady-flow problem, the initial flow corresponds to a uniform translation flow. For uniform rolling or rolling oscillation of a wing in a translating flow, the initial flow corresponds to a uniform translation plus the opposite rigid body rotation.

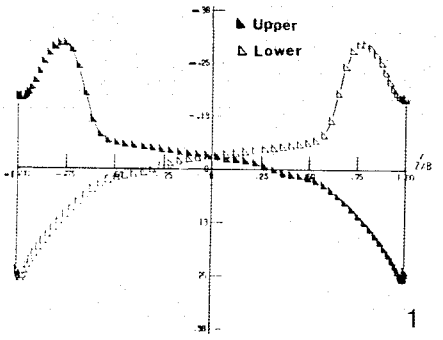

a) Surface pressure

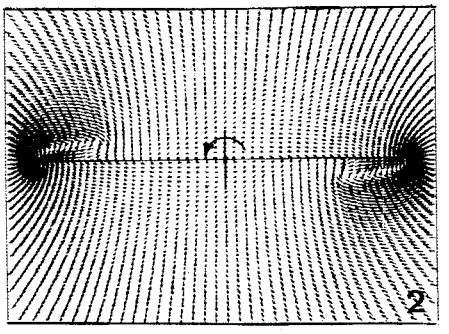

b) Crossflow velocity

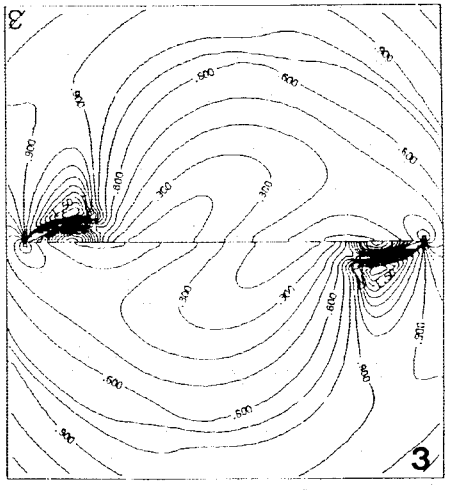

c) Crossflow Mach

Fig. 1 Uniform rolling of a delta wing, $M_\infty=2$, $\alpha=70$ deg, $\omega=0.5$.

Boundary Conditions

Since we are dealing with asymmetric flows in general, the symmetry condition has been removed, and the problem is solved over the whole of the computational domain, which includes the right and left regions to the plane of geometrical symmetry.

On the wing surface, the momentum equation in the normal direction to the surface is used to enforce the surface boundary condition. Substituting the conditions

$$\frac{D'}{Dt'}(V_r\cdot\hat{n})=0, \qquad \frac{\partial'\hat{n}}{\partial t'}=0 \tag{23}$$

in the normal momentum equation, we obtain the surface boundary condition

$$\frac{\partial p}{\partial n}=\rho V_r\cdot(V_r\cdot\nabla\hat{n})-\rho\hat{n}\cdot[2\,\dot{\bar{\omega}}xV_r+\dot{\bar{\omega}}xr+\dot{\bar{\omega}}x(\dot{\bar{\omega}}xr)] \tag{24}$$

where $\hat{n}$ is the unit normal to wing surface.

It should be noted that $(\partial'\hat{n}/\partial t')=0$ corresponds to the rigid-wing problem. For aeroelastic problems, $\partial'\hat{n}/\partial t'$ is calculated from the wing aeroelastic equation under the most recently calculated aerodynamic loads. Obviously in the latter problem iteration should be performed at each time step, or perhaps after each several time steps, to find the converged aerodynamic loads and the corresponding wing surface. This problem is a natural extension to the present rigid-wing problem.

In the far field and for supersonic conical flow problems, a uniform translation plus the rotation corresponding to the problem under consideration are imposed outside of the bow shock, which is captured as part of the solution.

Numerical Examples

A conical grid, which is obtained by using a modified Joukowski transformation,[4] of 128×64 cells around and normal to the wing, has been used for the whole computational region. The first numerical test is a code validation test in which a steady supersonic symmetric flow has been solved

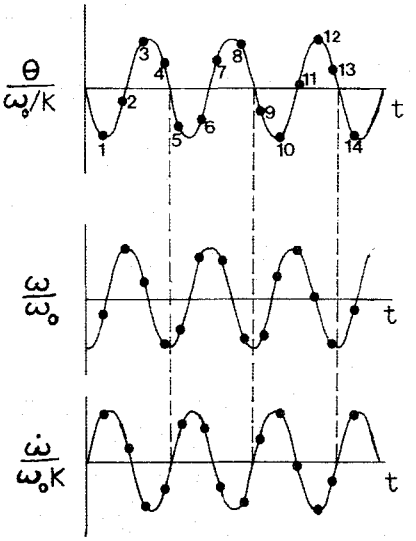

Fig. 2 Roll angle, angular speed, and angular acceleration of the rolling oscillation motion.

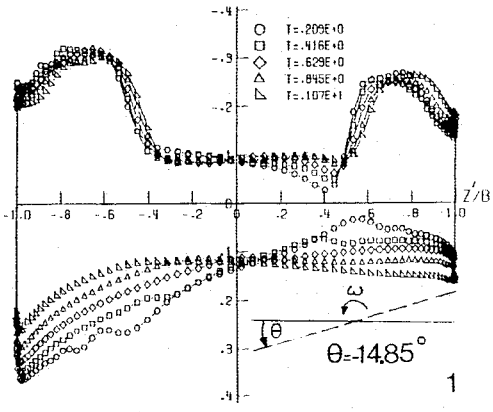

a) Surface pressure

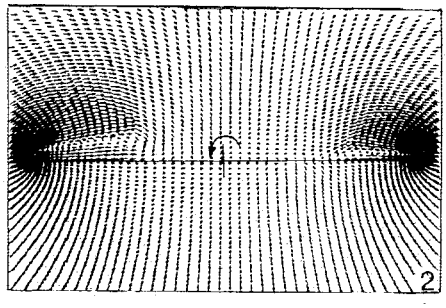

b) Crossflow velocity

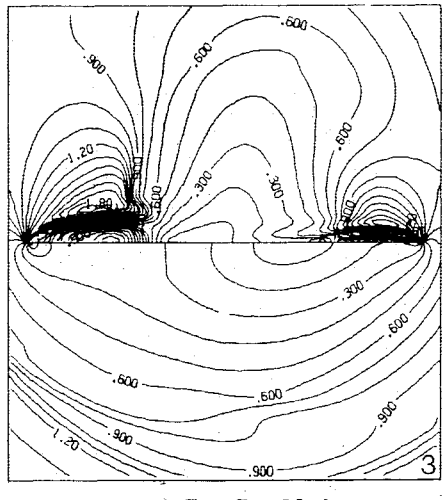

c) Crossflow Mach

Fig. 3 Rolling oscillation of a delta wing, $M_\infty = 2$, $\alpha = 10$ deg, $\beta = 70$ deg, $\omega = 0.35$, $k = 1.337$, $\theta_{max} = 15$ deg, $t = 0 - 1.07$, $\theta = 0 - (14.85$ deg).

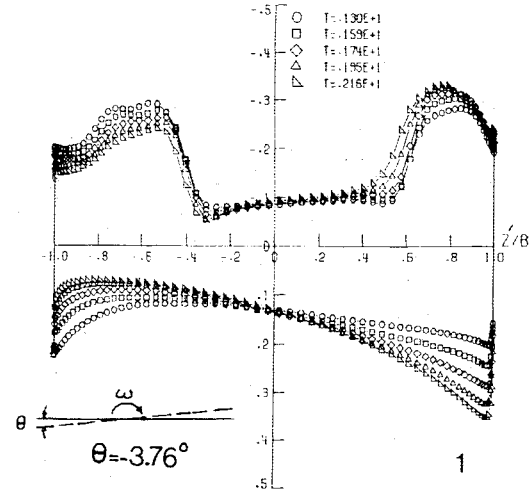

a) Surface pressure

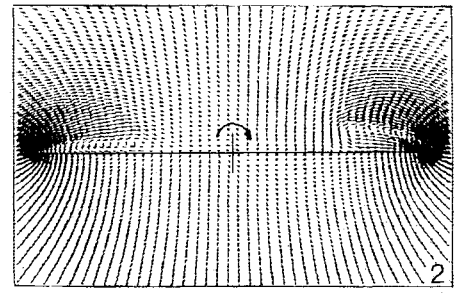

b) Crossflow velocity

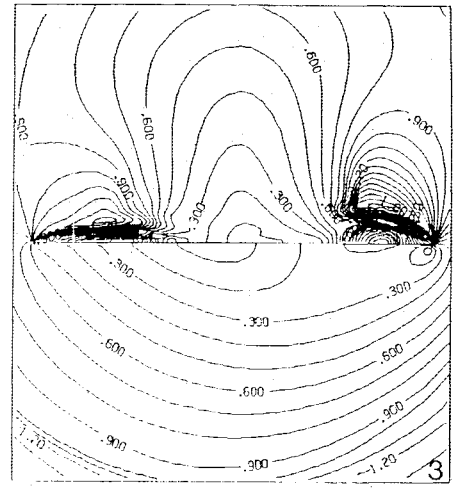

c) Crossflow Mach

Fig. 4 Rolling oscillation of a delta wing, $M_\infty = 2$, $\alpha = 10$ deg, $\beta = 70$ deg, $\omega = 0.35$, $k = 1.337$, $\theta_{max} = 15$ deg, $t = 1.07^+ - 2.16$, $\theta = (-14.85$ deg) $-$ (-3.76 deg).

for a sharp-edged delta wing at $M_\infty = 2$, $\alpha = 10$ deg, and β (sweep angle) = 70 deg. Two symmetric leading-edge vortices have been captured on the suction side along with a weak crossflow shock under each vortex. The outer bow shock has also been captured. The computed results of surface pressure, Mach contours, and static-pressure contours match those that were obtained by using the conical flow program for half of the computational region.[4] The results of this case are given in Ref. 24.

Having established confidence in the present computer program through this test and others, we consider asymmetric steady- and unsteady-flow problems.

Uniformly Rolling Wing in a Conical Flow

Figure 1 shows the results for a flat plate sharp-edged delta wing undergoing uniform rolling in the counterclockwise direction around its axis ox' at a constant angular speed $\omega = (\ell\omega^*/U_\infty) = 0.5$, where ω^* and ω are the dimensional and dimensionless angular speeds, ℓ the wing root chord, and U_∞ the freestream speed. The freestream Mach number and sweepback angle are $M_\infty = 2$ and $\beta = 70$ deg. The wing angle of attack is $\alpha = 0$, and hence the flow is steady in the rotating frame of reference. Figure 1a shows the upper "▲" and lower "△" surface pressure. As expected, the solution shows an exact antisymmetric surface pressure. Figures 1b and 1c show the corresponding crossflow velocity and crossflow Mach contours. On the crossflow Mach contours and under the antisymmetric leading-edge vortices, one notices a weak crossflow shock.

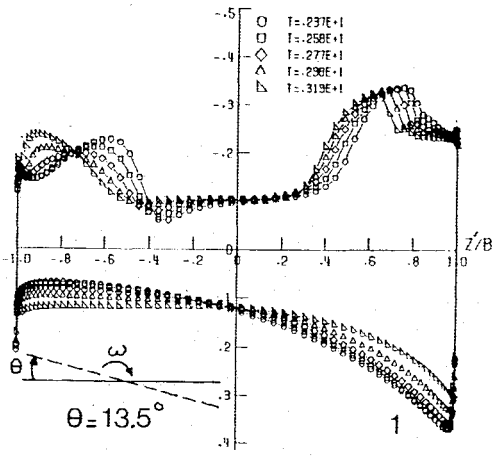

a) Surface pressure

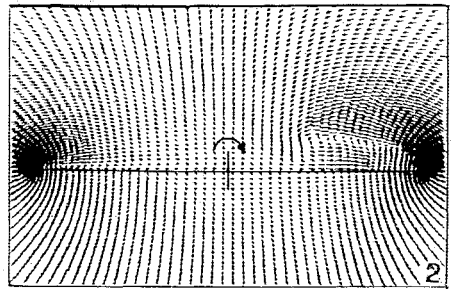

b) Crossflow velocity

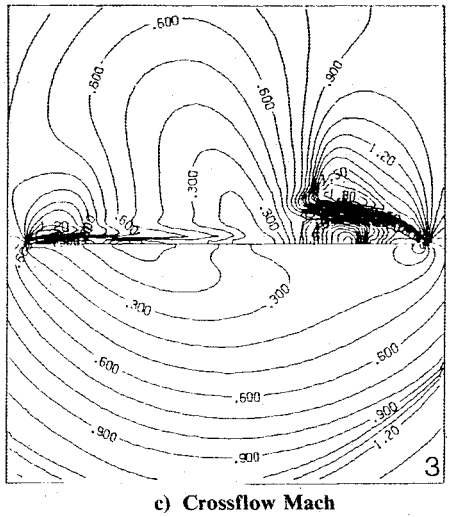

c) Crossflow Mach

Fig. 5 Rolling oscillation of a delta wing, $M_\infty = 2$, $\alpha = 10$ deg, $\beta = 70$ deg, $\omega = 0.35$, $k = 1.337$, $\theta_{max} = 15$ deg, $t = 2.16^+ - 3.19$, $\theta = (-3.76 \text{ deg}) - (+13.5 \text{ deg})$.

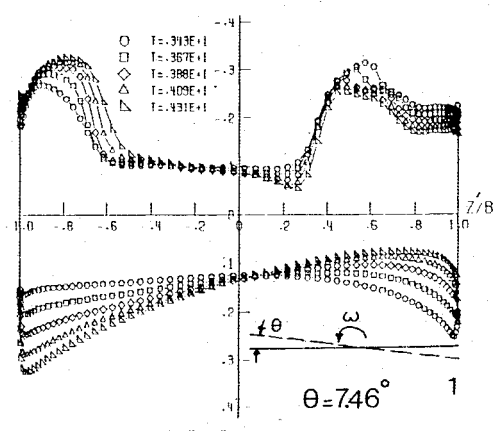

a) Surface pressure

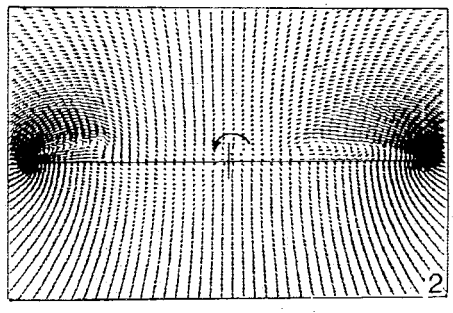

b) Crossflow velocity

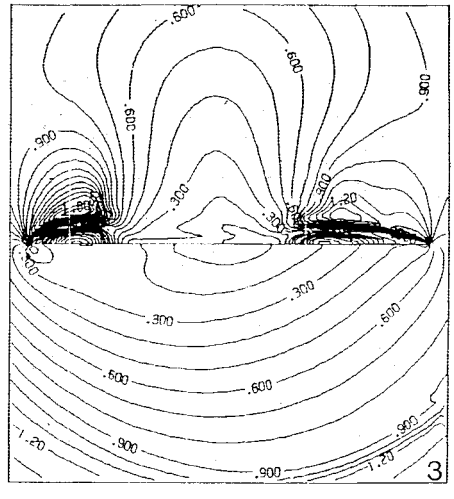

c) Crossflow Mach

Fig. 6 Rolling oscillation of a delta wing, $M_\infty = 2$, $\alpha = 10$ deg, $\beta = 70$ deg, $\omega = 0.35$, $k = 1.337$, $\theta_{max} = 15$ deg, $t = 3.19^+ - 4.31$, $\theta = (+13.5 \text{ deg}) - (+7.46 \text{ deg})$.

Rolling Oscillation of a Wing in a Locally Conical Flow

In this case, we consider the same flat-plate sharp-edged delta wing at $M_\infty = 2$, $\alpha = 10$ deg, and $\beta = 70$ deg. The wing is given a rolling sinusoidal oscillation of $\bar{\omega}$ and θ of $\bar{\omega} = -\omega_o \cos kt\, \hat{e}_{x'}$ and $\theta = -\theta_{max} \sin kt$, where $\theta_{max} = \omega_o/k$ and k is the dimensionless reduced frequency of oscillation [$K = (k^* \ell / U_\infty)$, k^* is the dimensional frequency]. Choosing $\theta_{max} = \pi/12$ and $\omega_o = 0.35$, the corresponding $k = 1.337$, and the period of oscillation $\tau = 4.699$. Throughout the time-accurate integration, the average value of the minimum global time step is approximately equal to 0.53×10^{-3}, and hence each cycle takes about 9000 time steps. It should be recalled that the computational scheme is explicit. The fully vectorized program takes about 1000 s of CPU time per cycle on the VPS-32 at NASA Langley Research Center. Figure 2 shows the rolling oscillation motion.

Figure 3 shows the results for the time range $t = 0 - 1.07$ (transient response). By the end of this time, the wing has rolled through an angle $\theta = -14.85$ deg, which corresponds to the end of the first quarter of the cycle (point 1 on Fig. 2). At $t = 0$, $\omega = \omega_o$, and ω decreases in the counterclockwise direction within that time. Figure 3a shows the surface pressure after each 400 time steps covering a total of 2000 time steps. On the upper surface, the suction pressure on the left is higher than that on the right, and the suction peak is moving in the spanwise direction in the positive z' direction. On the lower surface, the surface pressure is decreasing on the left side while it is increasing on the right side. Figures 3b and 3e show the crossflow velocity and crossflow Mach contours at $t = 1.07$ and $\theta = -14.85$ deg. At this moment, a large leading-edge vortex appears on the left, and a small leading-edge vortex appears on the right. The crossflow Mach

contours show shocks above and below the left leading-edge vortex. It also shows the outer bow shock with varying strength (lower portion of the figure).

Figure 4 shows the results for the time range $t = 1.07^{+} - 2.16$ (transient response). Within this time, the wing has reversed its direction of rotation (clockwise direction) with increasing ω, and by the end of this time the wing roll angle $\theta = -3.76$ deg (point 2 on Fig. 2). Figure 4a shows the surface pressure after each 400 time steps covering the range of time steps from 2001–4000. The peak suction pressure on the left is decreasing, corresponding to a decrease in size of the left vortex, while that on the right is increasing, corresponding to an increase in size of the right vortex. Figures 4b and 4c show the crossflow velocity and crossflow Mach contours at $t = 2.16$, $\theta = -3.76$ deg.

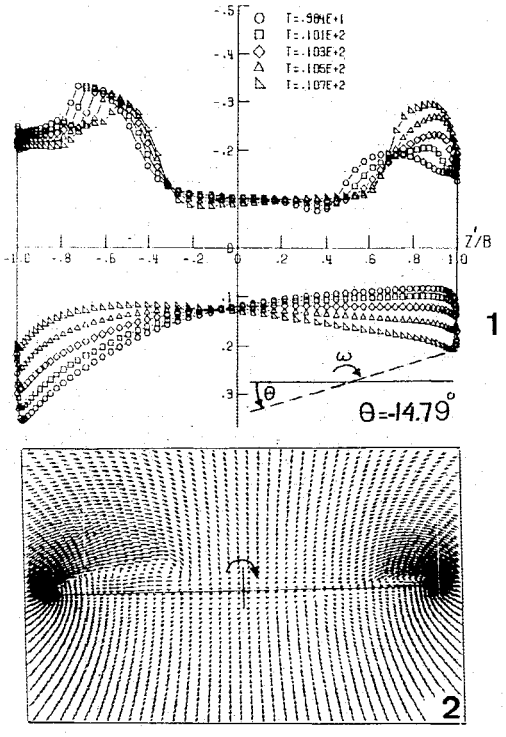

a) $t = 10.7$

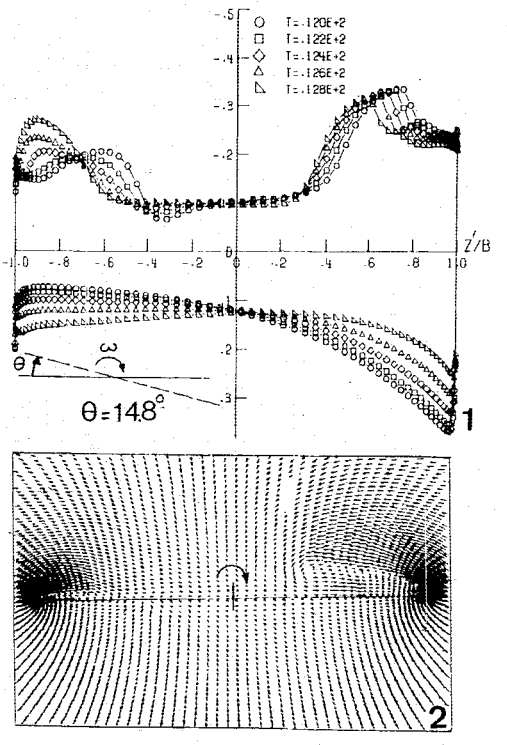

c) $t = 12.8$

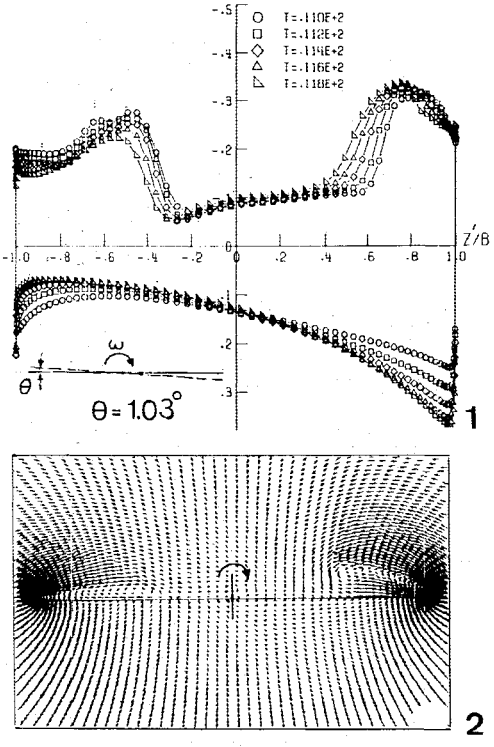

b) $t = 11.8$

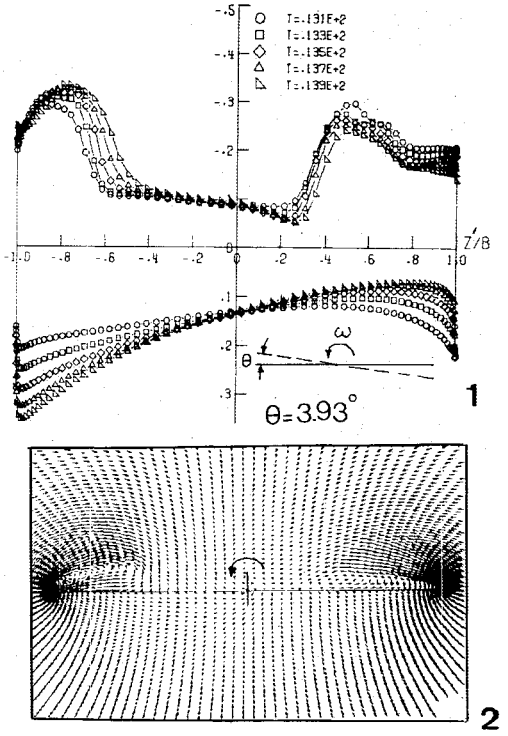

d) $t = 13.9$

Fig. 7 Rolling oscillation motion during periodic response (1 = surface pressure, 2 = crossflow velocity).

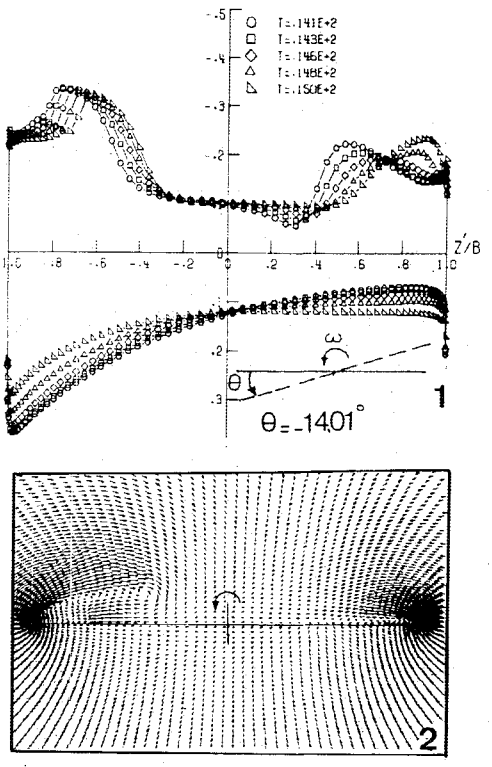

e) $t = 15$

Fig. 7 Continued.

Figure 5 shows the results for the time range $t = 2.16^+ - 3.19$, (transient response) during which the wing is rotating in the clockwise direction with decreasing ω. By the end of this time, the roll angle is $\theta = 13.5$ deg (point 3 on Fig. 2). Figure 5a shows the surface pressure covering the range of time steps 4001–6000. The peak suction pressure on the left is moving to the left as the vortex is disappearing, and an attached flow is developing. The peak suction pressure on the right is moving inboard to the left, while the shock under the vortex is growing. Figures 5b and 5c show the crossflow velocity and crossflow Mach contours at $t = 3.19$ and $\theta = 13.5$ deg.

Figure 6 shows the results for the time range $t = 3.19^+ - 4.31$ (transient response) during which the wing has reversed the direction of rotation from clockwise to counterclockwise, and ω has reached a zero value and then increases. The vortex on the left is growing, and the corresponding peak suction pressure is increasing and moving inboard to the right. The vortex on the right is flattening, and its peak suction pressure is decreasing and moving inboard to the left. By the end, this time $t = 4.31$, the roll angle $\theta = 7.46$ deg (point 4 on Fig. 2).

Within the time range $t = 4.31^+ - 5.35$, the wing is still rotating in the counterclockwise direction, and ω has reached its maximum value and then decreases. At $t = 4.7$, the wing has already completed one cycle of oscillation.

Figures 7a–7e show the results during the periodic response (points 10–14 on Fig. 2) covering the ranges of time steps 20,001–28,000. The results show the successive increase, decrease, and motion of the left and right vortices, and their corresponding peak suction pressure. They also show the formation and disintegration of the shocks below and above the vortices and the motion and strength variation of the outer bow shock.

Figure 8 shows a summary of the surface pressure variation during a typical periodic response.

Figure 9 shows the time history of the lift and rolling-moment coefficients along with roll angle variation. Steady-state oscillation response is reached by the third cycle. While

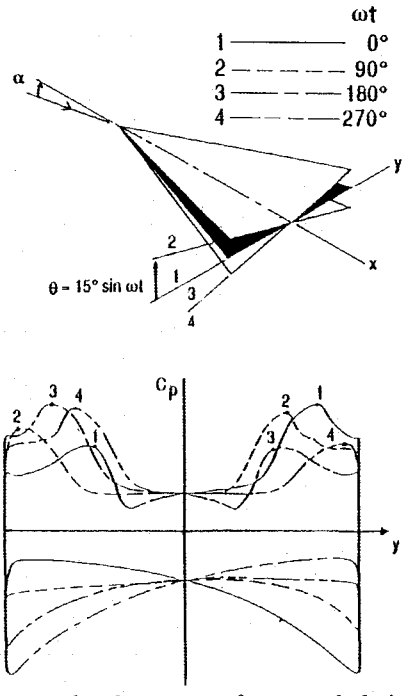

Fig. 8 Summary of surface pressure for one cycle during the periodic response.

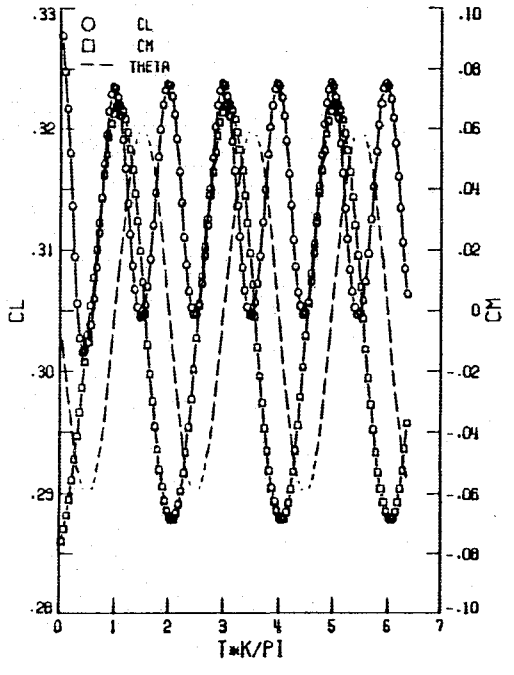

Fig. 9 The history of the lift and rolling-moment coefficients.

the phase angle between C_M and θ is 90 deg, C_M is in phase with ω. Although C_M and θ have the same frequency, C_L shows twice the value of that frequency.

Concluding Remarks

A three-dimensional fully vectorized computer program has been developed to solve for the steady and unsteady maneuvering delta wings. The unsteady Euler equations for the flow relative motion in a rotating frame of reference have been derived in the strong conservation form. The resulting equations have been solved by using the central-difference

finite-volume scheme with four-stage Runge-Kutta time stepping. The present formulation, where the computational grid is carried with the moving frame of reference, does not require, for rigid wings, any additional computations of the grid motion. For aeroelastic problems, where the wing is deforming and the deformations are usually small, the computation of the grid deformation will be required after each several time steps.

The numerical results covered three cases (two cases are shown in this paper): a steady symmetric conical flow, a steady antisymmetric conical flow (uniform rolling at zero angle of attack), and an unsteady asymmetric locally conical flow (rolling oscillation). The present program can treat three-dimensional flows around wings in pitching, yawing, rolling, and heaving oscillations including aeroelastic deformations over a wide range of Mach numbers and angles of attack. Currently, the explicit scheme is replaced by an implicit one to further reduce to the computational time. Extension of this program to the Navier-Stokes equations is straightforward. This is the first time, that we know of, to solve for an unsteady vortex-dominated delta wing problem, including shocks, using Euler equations and the CFD schemes.

Acknowledgment

This research work has been supported by NASA Langley Research Center under Grant NAG-1-648.

References

[1]Miller, D. S. and Wood, R. W., "Lee-Side Flow Over Delta Wings at Supersonic Speed," NASA TP-2430, 1985.

[2]Newsome, R. W., "A Comparison of Euler and Navier-Stokes Solutions for Supersonic Flow Over a Conical Delta Wing," *AIAA Journal*, Vol. 24, April 1986, pp. 552-561.

[3]Powell, K., Murman, E., Perez, E., and Baron, J., "Total Pressure Loss in Vortical Solutions of the Conical Euler Equations," *AIAA Journal*, Vol. 25, March 1987, pp. 360-368.

[4]Kandil, O. A. and Chuang, A. H., "Influence of Numerical Dissipation in Computing Supersonic Vortex-Dominated Flows," *AIAA Journal*, Vol. 25, Nov. 1987, pp. 1426-1434.

[5]Rizzi, A., "Three-Dimensional Solutions to Euler Equations with One Million Grid Points," *AIAA Journal*, Vol. 23, Dec. 1985, pp. 1986-1987.

[6]Newsome, R. W. and Adams, M. S., "Numerical Simulation of Vortical-Flow Over an Elliptical-Body Missile at High Angles of Attack," AIAA Paper 86-0559, Jan. 1986.

[7]Rizetta, D. P. and Shang, J. S., "Numerical Simulation of Leading Edge Vortex Flows," *AIAA Journal*, Vol. 24, Feb. 1986, pp. 237-245.

[8]Thomas, J. L. and Newsome, R. W., "Navier-Stokes Computations of Lee-Side Flows Over Delta Wings," AIAA Paper 86-1049, May 1986.

[9]Kandil, O. A., Chuang, A. H., and Shifflette, J. M., "Finite-Volume Euler and Navier-Stokes Solvers for Three-Dimensional and Conical Vortex Flows Over Delta Wings," AIAA Paper 87-0041, Jan. 1987.

[10]Thomas, J. L., Taylor, S. L., and Anderson, W. K., "Navier-Stokes Computations of Vortical Flows Over Low Ratio Wings," AIAA Paper 87-0207, Jan. 1987.

[11]Lin, C. H., Hsu, C. H., and Hartwich, P. M., "Incompressible Navier-Stokes Solutions for a Sharp-Edged Double-Delta Wing," AIAA Paper 87-0206, Jan. 1987.

[12]Newsome, R. W. and Kandil, O. A., "Vortex Flow Aerodynamics—Physical Aspects and Numerical Simulations," AIAA Paper 87-0205, Jan. 1987.

[13]Edwards, J. W., Bland, S. R., and Seidel, D. A., "Experience with Transonic Unsteady Aerodynamic Calculations," AGARD CP-374, Jan. 1985.

[14]Batina, J. T., "Unsteady Transonic Flow Calculations for Wing-Fuselage Configurations," AIAA Paper 86-0862, May 1986.

[15]Whitlow, W., Jr., Hafez, M. H., and Osher, S. J., "An Entropy Correction Method for Unsteady Fall Potential Flows with Strong Shocks," AIAA Paper 86-1768-CP, June 1986.

[16]Ruo, S. Y., Malone, J. B., and Sankar, L. N., "Steady and Unsteady Calculations for High and Low Aspect Ratio Supercritical Wings," AIAA Paper 86-0122, Jan. 1986.

[17]Shanker, V. and Ide, H., "Full Potential Unsteady Computations Including Aeroelastic Effects," Transonic Unsteady Aerodynamics Symposium, NASA Langley Research Center, Hampton, VA, May 1987.

[18]Belk, D., Janus, J., and Whitfield, D., "Three-Dimensional Unsteady Euler Equations Solutions on Dynamic Grids," AIAA Paper 85-1704, July 1985.

[19]Ruo, S. Y. and Sankar, L. N., "Solution of Unsteady Rotational Flow Over Supercritical Wings," AIAA Paper 87-0108, Jan. 1987.

[20]Anderson, K. W., Thomas, J. L., and Rumsy, C. L., "Flux-Vector Splitting for Unsteady Calculations on Dynamic Meshes," Transonic Unsteady Aerodynamics Symposium, NASA Langley Research Center, Hampton, VA, May 1987.

[21]Shamroth, S. J., "Calculation of Steady and Oscillating Airfoil Flow Fields via the Navier-Stokes Equations," AIAA Paper 84-525, Jan. 1984.

[22]Rumsey, C. L., Anderson, K. W., and Thomas, J. L., "Unsteady Turbulent Navier-Stokes Computations Over the NACA 0012 Airfoil," Transonic Unsteady Aerodynamics Symposium, NASA Langley Research Center, Hampton, VA, May 1987.

[23]Edwards, J. W. and Thomas, J. L., "Computational Methods for Unsteady Transonic Flows," AIAA Paper 87-0107, Jan. 1987.

[24]Kandil, O. A. and Chuang, A. H., "Computation of Steady and Unsteady Vortex Dominated Flows," AIAA Paper 87-1462, June 1987.